

## Pressure-Induced Transformation Path of Graphite to Diamond

S. Scandolo, M. Bernasconi,\* G. L. Chiarotti, P. Focher, and E. Tosatti  
*International School for Advanced Studies, Via Beirut 4, I-34014 Trieste, Italy*  
 (Received 13 December 1994)

Using constant-pressure *ab initio* molecular dynamics we have simulated the conversion of carbon from graphite to diamond under high pressure. We found that the transformation path proceeds through sliding of graphite planes into an unusual orthorhombic stacking, from which an abrupt collapse and buckling of the planes leads to both cubic and hexagonal forms of diamond in comparable proportions. The mutual orientation of the initial and final phases is in agreement with that of shock-wave experiments.

PACS numbers: 62.50.+p, 64.70.Kb, 81.30.Hd

Understanding the dense phases of carbon, and the mechanisms which underlie their mutual transformations, is a long-standing problem of great practical and fundamental importance. Although hexagonal graphite (hex-g) is known to be the most stable phase of carbon at ambient conditions, a large activation barrier prevents cubic diamond (cub-d) from transforming, even on a geological time scale, to graphite. Since the high-pressure region of the carbon phase diagram is instead dominated by diamond [1], methods devised to convert graphite into diamond rely on the use of high pressure [2]. After the first report [3] on the shock-wave conversion of graphite to diamond without catalyst, there is now general agreement that the conversion takes place even statically at a pressure of  $\sim 15$  GPa and at temperatures exceeding 1000 K [2]. Instead, agreement is far from complete on the conversion mechanism. In particular, the role of hexagonal diamond (Lonsdaleite), first synthesized under similar experimental conditions [4], is not clear. A number of reports indicate that, although metastable with respect to cub-d, hexagonal diamond (hex-d) may be produced through rapid quenching of shocked samples [2], or even in static high-pressure conditions [5]. However, recent attempts to reproduce the graphite to hex-d conversion under static conditions failed [6]. The relevance of hex-d in the graphite to cub-d conversion appears to be twofold. First, the mutual orientation of graphite and cub-d before and after the conversion process is consistent with the presence of hex-d as an intermediate phase [2]. Secondly, hex-d was observed *in situ* in a recent x-ray diffraction experiment at high pressure [7], but after heating and quenching to room conditions, only cub-d could be retrieved. More generally, the existence of an intermediate phase has often been invoked [5,8,9], but never been substantiated.

From the theoretical side, only the highly symmetric path from rhombohedral graphite (rho-g) (Fig. 1) to cub-d has been considered [10,11]. This path leads to a final [111] diamond orientation *parallel* to the original graphite *c* axis [Fig. 2(a)]. This is at variance with shock-wave experiments, where the final [112] is instead found to be parallel to the *c* axis [12] [Fig. 2(b)]. The relative

crystal-axes orientation is a particularly revealing feature of the transformation path which has not been addressed theoretically so far.

In this Letter we present the results of an *ab initio* molecular dynamics (MD) simulation of the graphite to diamond conversion. They have been obtained by using a recently developed *ab initio* constant-pressure simulation method [13], where the lack of symmetry constraints is crucial in allowing for possible low-symmetry transformation paths. We find that pressure eventually causes a sliding of graphite planes towards an orthorhombic stacking, from which a fast transformation to both hexagonal and/or cubic diamond takes place.

A Car-von Barth atomic pseudopotential for carbon in the Kleinman-Bylander form was used [14], and the sampling of the Brillouin zone was restricted to the  $\Gamma$  point. Because of the hardness of carbon pseudopotential and the large volume reduction expected in the compression of graphite, a corrected version of the kinetic energy functional was introduced in order to mimic a constant energy cutoff of 35 Ry in the plane-wave expansion of the ground state at different volumes [15]. Although full convergence cannot be claimed at 35 Ry, the basic chemistry and crystal binding is quite well described. For example, with this choice bond lengths in carbon clusters are accurate within a few percent [14]. The equations of motion have been

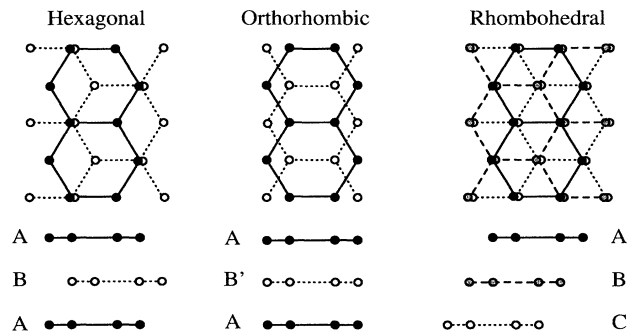


FIG. 1. Hexagonal, orthorhombic, and rhombohedral phases of graphite. The different stackings of the hexagonal planes are viewed along the *c* axis (above) and sideways (below).

“preconditioned” by introducing different masses for different plane-wave components [16], allowing the use of an integration step of 6 a.u. ( $1.45 \times 10^{-4}$  ps).

We carried out a total of four distinct simulation runs, based on differently chosen initial conditions and starting cells containing 48 or 64 atoms. All simulations started with hexagonal graphite, and the choice of each cell was such as to minimize the zero-pressure ground-state energy at the experimental lattice spacings ( $a = 2.461$  Å,  $c/a = 2.726$ ) [17]. The cells were then allowed to relax to their equilibrium shape. This led to negligible variations of  $a$  (<2%) and to a maximum contraction of ~12% of the  $c/a$  parameter. The total energy of graphite in the starting cells was found in all cases to be close, within ~50 meV/atom, to that of cubic diamond. Hence, the two phases are practically degenerate, and pressure is needed only to overcome the barrier between them.

Figure 3 sketches the history of a 48-atom simulation on the energy versus volume diagram. Graphite was first compressed up to a pressure of 30 GPa at  $T = 200$  K. Initially, the *ABAB* stacking of hex-g slowly changed to the *AB'AB'* stacking of orthorhombic graphite (ort-g), shown in Fig. 1. Although ort-g is not found in nature, its possible relevance had been foreshadowed in the early literature, since most high-pressure phases of carbon appear to be connected by high-symmetry paths to ort-g [18–21].

In order to mimic the experimental procedure of quenching down to ambient conditions only after heating

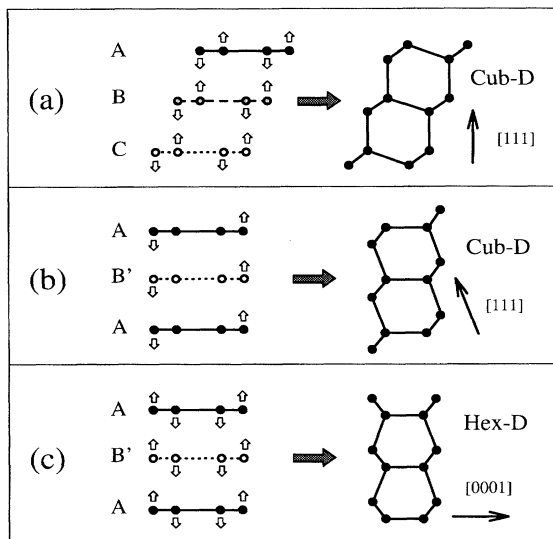


FIG. 2. Geometric paths for graphite  $\rightarrow$  diamond transformation: (a) rhombohedral graphite to cubic diamond; (b) orthorhombic graphite to cubic diamond; (c) orthorhombic graphite to hexagonal diamond. Depending on the stacking of graphite, the graphite  $c$  axis coincides with [111] of cubic diamond in (a), or with [112] of cubic diamond in (b), or with [1210] of hexagonal diamond in (c). Atomic displacements from the graphite basal planes are shown on the left by the arrows.

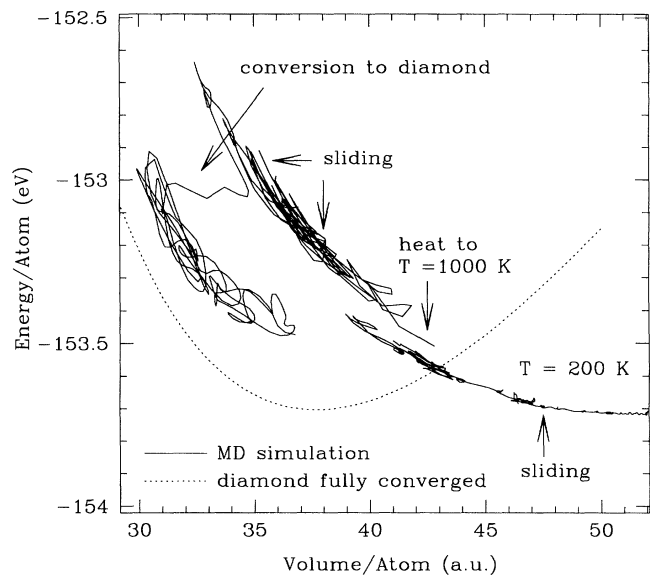


FIG. 3. Energy vs volume diagram (solid line) of the graphite  $\rightarrow$  cubic diamond transformation, as obtained by the MD simulation with the 48-atom cell. The zero-temperature equation of state of ideal cubic diamond computed at convergence in  $K$  point sampling is also reported (dotted line). The simulation starts with hex-g (right side) and ends with cub-d (left side).

to 1000–2000 K during the compression, we have heated, at this point, our crystal up to 1000 K. Pressure was then increased at a faster rate ( $\sim 300$  GPa/ps). At  $P \sim 60$  GPa, the graphite reverted back to hexagonal, and at  $P \sim 90$  GPa again to orthorhombic. The mobility of the graphitic planes suggests not only closeness in energy of different stackings but also a lack of barrier between them, even at high pressure. We then let the system run for about 0.2 ps, at which point ort-g suddenly converted into cubic diamond. The conversion took place, as in the case of silicon [13], at a very high value of the applied pressure (here 90 GPa, against an experimental estimate of 15 GPa [5]). It carried through bodily without the formation of defects, a process allowed by a deformable cell. The interplanar distance in graphite first collapsed, leading to a buckling of the graphitic basal planes. Next, the buckled planes suddenly gave up their  $\pi$  electrons and became bonded to one another, turning into (111) diamond planes, the [0001] direction of the original graphite phase becoming the [112] of diamond, as shown in Fig. 2(b). The conversion from ort-g to diamond took place in an overall time of  $\sim 10^{-2}$  ps.

We finally released the pressure in order to follow the equation of state and compare it with that of ideal cub-d (dotted line in Fig. 3). The latter was accurately computed with ten special points in the irreducible Brillouin zone (BZ). The  $\sim 0.2$  eV/atom energy difference in the two equations of state can be traced back both to the  $\Gamma$  point sampling of our supercell ( $\sim 0.1$  eV/atom) and to thermal motion ( $\sim 0.1$  eV/atom).

In order to check on the possible role of temperature in the transformation, a second simulation was performed with the same 48-atom initial cell, but keeping the temperature at the initial value of  $\sim 200$  K. No significant differences in the transformation path were found with respect to the first simulation, apart from the transition pressure, which was found to be slightly higher (110 GPa).

The formation of hex-d was not observed in either of these 48-atom simulations. However, considering the transformation path involving ort-g, out of a total of three geometrically equivalent directions through which the conversion of hex-g to cub-d or hex-d may occur, only one is allowed in a 48-atom cell for the hex-g  $\rightarrow$  hex-d while all three are allowed for hex-g  $\rightarrow$  cub-d. Therefore we decided to carry out another simulation with a different cell, chosen so as to allow all the three hex-d buckling paths. This was possible with a 64-atom cell which has the additional virtue of a better  $k$  point sampling of the initial ideal hex-g crystal. Two different runs were performed with this cell, at 1500 and 150 K, respectively. Pressure was increased at a rate of  $\sim 80$  GPa/ps in both cases. The graphite planes again displayed high mobility and again shifted to the ort-g stacking. At this point the conversion process proceeded differently in the two runs. In the high temperature case hex-d was obtained, with the same orientation relative to hex-g observed in experiments [5]. A phonon analysis [22] of hex-d on our trajectories after releasing the system to zero pressure gives two Raman-active peaks at 1237 and 1306  $\text{cm}^{-1}$ . The latter is in reasonable agreement with the cub-d Raman frequency of 1332  $\text{cm}^{-1}$ . The lowest mode instead can be identified with a signature of hex-d, seen at 1170  $\text{cm}^{-1}$ , as recently proposed [23]. The low temperature run is also interesting, and is presented in Fig. 4, where four snapshots of the atomic positions taken at intermediate times are shown. Sliding of the graphite layers from the hex-g stacking [Fig. 4(a)] to the ort-g stacking [Fig. 4(b)] occurred after 1 ps from the beginning of the simulation. The next two snapshots are taken 0.01 and 0.02 ps after Fig. 4(b), respectively. Buckling of the planes is accompanied by the formation of  $sp^3$  bonds connecting the graphite planes [Fig. 4(c)], and the  $sp^3$ -coordinated crystal shown in Fig. 4(d) is finally recovered. Because of the periodic boundary conditions of our cell, this crystal can be seen either as a sum of two twin domains of cub-d with a (111) hex-d-like stacking fault [dotted line in Fig. 4(d)], or as a sum of two twin domains of hex-d with a (0001) cub-d-like boundary plane (dashed line). Since in this defected structure the local atomic coordination is identical to that of cub-d, including the third nearest-neighbor, its energy cost must be comparable to the energy difference between cub-d and hex-d (which also differ in their fourth nearest-neighbor), and therefore very low [24].

We are now in a position to discuss and analyze the overall meaning of these simulation results. The

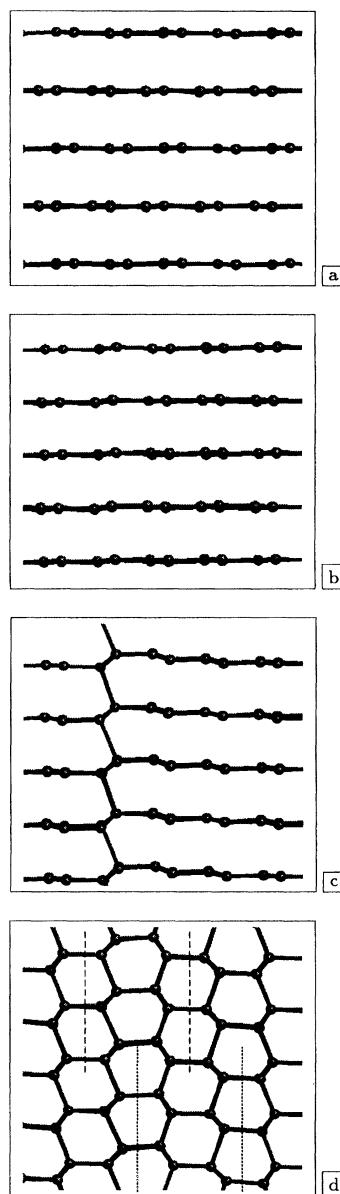


FIG. 4. Snapshots of the atomic positions at different intermediate times of the 64-atom low-temperature simulation. (a) compressed hexagonal graphite (1.0 ps); (b) after sliding to orthorhombic graphite (1.07 ps); (c) intermediate state of the conversion process with a single diamond bilayer (1.08 ps); (d) fully transformed diamondlike  $sp^3$ -coordinated structure (1.09 ps). This structure can be seen alternatively as a cubic-diamond or as a hexagonal-diamond twin-defected crystal. Cubic-diamond (hexagonal-diamond) twin boundaries are indicated by dotted (dashed) lines.

main feature, common to all of them, is the sliding of the graphite planes towards the ort-g stacking. In this stacking the planes can become chair buckled and yield cub-d [Fig. 2(b)], with the [112] axis parallel to the former  $c$  axis. Alternatively, they can become boat buckled,

yielding hex-d, whose new  $c$  axis is parallel to the initial [120] of hex-g, and therefore orthogonal to the graphite  $c$  axis [Fig. 2(c)]. The role of the intermediate ort-g phase, first hypothesized by Kurdyumov [18], is therefore strikingly confirmed, although we find no clear indication of a *stable* intermediate phase with this symmetry [25].

The two possible diamond structures, cub-d and hex-d, appear with very similar probabilities, or even coexist, in our simulations. This is most likely connected with the extreme abruptness of the transition, a situation which is possibly close to being realized in shock-wave experiments, where, in fact, both phases are found, precisely with the crystal orientation we find [2,12]. Runs at different compression rates (80 and 300 GPa/s) seem to indicate that the formation of cub-d is favored at the highest rates. Temperature instead does not play a relevant role in our simulations, probably due to the overwhelming effect of pressure fluctuations.

The mutual orientation of crystals before and after transformation is quite instructive. Parallelism of the [111] axis of cub-d with the  $c$  axis of graphite, found in the catalyst-aided conversion [26], never appears in our simulations. Since the use of metal catalysts is also known to drastically decrease the transition pressure, and is therefore expected to alter significantly the conversion mechanism (possibly through a metal-induced buckling of the graphitic basal planes [2]), we do not expect agreement between our simulation and the catalyst-aided conversion. By contrast, the orientation of hex-d and of cub-d obtained by shock-wave conversion, relative to the initial axes of hex-g, are only rationalized through our transformation path, which receives, therefore, strong support.

In conclusion, we have demonstrated the ability of *ab initio* molecular dynamics to simulate the pressure-induced transformation of graphite to diamond and to clarify at least the intermediate stages of the transformation path. The absence of symmetry constraints in our simulation turns out to be crucial in permitting a transformation path never considered theoretically so far. The path is consistent with the mutual orientation observed in shock-wave experiments and accounts for the appearance of both cub-d and hex-d in the conversion products.

---

\*Present address: Max-Planck-Institut für Festkörperforschung, Heisenbergstrasse 1, D-70506 Stuttgart, Germany.

[1] F. P. Bundy, *Physica* (Amsterdam) **156A**, 169 (1989).

- [2] R. Clarke and C. Uher, *Adv. Phys.* **33**, 469 (1984).  
 [3] P. S. DeCarli and J. C. Jameson, *Science* **133**, 1821 (1961).  
 [4] R. B. Aust and H. G. Drickamer, *Science* **140**, 817 (1963).  
 [5] F. P. Bundy and J. S. Kasper, *J. Chem. Phys.* **46**, 3437 (1967).  
 [6] S. Endo, N. Idani, R. Oshima, K. J. Takano, and M. Wakatsuki, *Phys. Rev. B* **49**, 22 (1994).  
 [7] T. Yagi, W. Utsumi, M. Yamakata, T. Kikegawa, and O. O. Shimomura, *Phys. Rev. B* **46**, 6031 (1992).  
 [8] K. J. Takano, H. Harashima, and M. Wakatsuki, *Jpn. J. Appl. Phys.* **30**, L860 (1991).  
 [9] W. Utsumi and T. Yagi, *Science* **252**, 1542 (1991).  
 [10] S. Fahy, S. G. Louie, and M. L. Cohen, *Phys. Rev. B* **35**, 7623 (1987).  
 [11] M. Kertesz and R. Hoffmann, *J. Solid State Chem.* **54**, 313 (1984).  
 [12] E. J. Wheeler and D. Lewis, *Mat. Res. Bull.* **10**, 687 (1975).  
 [13] P. Focher, G. L. Chiarotti, M. Bernasconi, E. Tosatti, and M. Parrinello, *Europhys. Lett.* **36**, 345 (1994).  
 [14] W. Andreoni, D. Sharf, and P. Giannozzi, *Chem. Phys. Lett.* **173**, 449 (1990).  
 [15] M. Bernasconi, G. L. Chiarotti, P. Focher, S. Scandolo, E. Tosatti, and M. Parrinello, *J. Phys. Chem. Solids* (to be published).  
 [16] F. Tassone, F. Mauri, and R. Car, *Phys. Rev. B*, **50**, 10561 (1994).  
 [17] Because of the  $\Gamma$  point sampling, different cells yield slightly different ground-state energies. The minimum-energy cell avoids unphysical transitions between different cells.  
 [18] A. V. Kurdyumov, *Sov. Phys. Dokl.* **20**, 218 (1975).  
 [19] A. V. Kurdyumov, N. F. Ostrovskaya, A. N. Pilyankevich, and I. N. Frankevich, *Sov. Phys. Dokl.* **23**, 278 (1978).  
 [20] V. A. Zhorin, M. Ya. Kushnerev, D. P. Shashkin, V. G. Nagorny, and N. S. Enikolopyan, *Russian J. Phys. Chem.* **56**, 1522 (1982).  
 [21] C. Mailhot and A. K. McMahan, *Phys. Rev. B* **44**, 11578 (1991).  
 [22] J. Kohanoff, *Comput. Mater. Sci.* **2**, 221 (1994).  
 [23] S. R. P. Silva, G. A. J. Amaratunga, E. K. H. Salje, and K. M. Knowles, *J. Mater. Sci.* **29**, 4962 (1994).  
 [24] S. Fahy and S. G. Louie, *Phys. Rev. B* **36**, 3373 (1987).  
 [25] The total energies of the three stackings of graphite at full convergence in BZ integration are degenerate within the accuracy of our calculation (10 meV/atom) up to a pressure of 80 GPa.  
 [26] L. F. Vereshchagin, Y. A. Kalashnikov, E. M. Feklichev, I. V. Nikolskaya, and L. M. Tikhomirova, *Sov. Phys. Dokl.* **10**, 534 (1965).